II CONGRESSO NACIONAL DE ENGENHARIA MECÂNICA
II NATIONAL CONGRESS OF MECHANICAL ENGINEERING
12 a 16 de Agosto de 2002 - João Pessoa – PB

NUMERICAL SIMULATION OF TURBULENT FLOWS USING THE MULTIGRID METHOD AND A LINEAR EDDY VISCOSITY MODEL

Maximilian Serguei Mesquita
Marcelo J.S. De-Lemos*
Departamento de Energia, IEME
Instituto Tecnológico de Aeronáutica – ITA
12228-900 - São José dos Campos, SP – Brazil
* E-mail: delemos@mec.ita.br

Abstract. *.The present work investigates the efficiency of the multigrid numerical method applied to solve two-dimensional turbulent velocity and temperature fields inside a rectangular domain. Numerical analysis is based on the finite volume discretization scheme applied to structure orthogonal regular meshes. Performance of the correction storage (CS) multigrid algorithm is compared for different inlet Reynolds number and number of grids. Up to four grids were used for both V- and W- cycles. Simultaneous and uncoupled temperature-velocity solution schemes were also applied.. Advantages in using more than one grid is discussed. Results further indicate an increase in the computational effort for higher* Re_{in} *and an optimal number of relaxation sweeps for both V- and W-cycles.*

Key-words: *Multigrid ,Converge acceleration, Non-isothermal flow*

1. INTRODUCTION

In most iterative numerical solutions, convergence rates of single-grid calculations are greatest in the beginning of the process, slowing down as the iterative process goes on. Effects like those get more pronounced as the grid becomes finer. Large grid sizes, however, are often needed when resolving small recirculating regions or detecting high heat transfer spots. The reason for this hard-to-converge behavior is that iterative methods can efficiently smooth out only those Fourier error components of wavelengths smaller than or comparable to the grid size. In contrast, multigrid methods aims to cover a broader range of wavelengths through relaxation on more than one grid.

The number of iterations and convergence criterion in each step along consecutive grid levels visited by the algorithm determines the cycling strategy, usually a V- or W-cycle. Within each cycle, the intermediate solution is relaxed before (*pre-*) and after (*post-smoothing*) the transportation of values to coarser (*restriction*) or to finer (*prolongation*) grids (Brandt, 1977, Stüben & Trottenberg, 1982, Hackbusch, 1985).

Accordingly, multigrid methods can be roughly classified into two major categories. In the CS formulation, algebraic equations are solved for the corrections of the variables whereas, in the full approximation storage (FAS) scheme, the variables themselves are handled in all grid levels. It has been pointed out in the literature that the application of the CS formulation is recommended for the solution of linear problems being the FAS formulation more suitable to non-linear cases (Brandt, 1977, Stüben & Trottenberg, 1982, Hackbusch, 1985). An exception to this rule seems to be the work of Jiang, et al, (1991), who reported predictions for the Navier-Stokes equations successfully

applying the multigrid CS formulation. In the literature, however, not too many attempts in solving non-linear problems with multigrid linear operators are found.

Acknowledging the advantages of using multiple grids, Rabi & de Lemos, 1998a, presented numerical computations applying this technique to recirculating flows in several geometries of engineering interest. There, the correction storage (CS) formulation was applied to non-linear problems. Later, Rabi & de Lemos, 1998b, 2001, analyzed the effect of Peclet number and the use of different solution cycles when solving the temperature field within flows with a given velocity distribution. In all those cases, the advantages in using more than one grid in iterative solution was confirmed, futhermore, de Lemos & Mesquita, 1999, introduced the solution of the energy equation in their multigrid algorithm. Temperature distribution was calculated solving the whole equation set together with the flow field as well as uncoupling the momentum and energy equations. A study on optimal relaxation parameters was there reported.

More recently Mesquita & De Lemos, 2000a, 2000b analyzed the influence of the increase of points of the mesh and optimal values of the parameters of the Multigrid cycle for different geometrias.

The present contribution extends the early work on CS multigrid methods to the solution of energy equation. More specifically, heated steady-state Turbulent flows in a heated tank are calculated with up to 3 grids. A schematic of such configurations is show in Figure **1** .

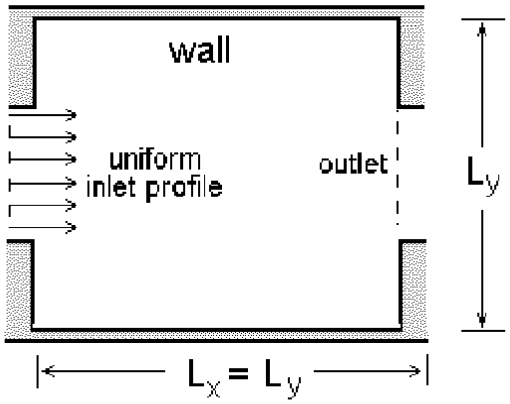

Figure 1 - Geometries and boundary conditions for heated tank flow

2. ANALYSIS

2.1. Governing Equations and Numerics

Governing Equations The continuity, Navier-Stokes and energy equations describe fluid flow and heat transfer. They express mass, momentum and energy conservation principles respectively and, for a steady state condition in a two-dimension Cartesian coordinate frame, they written as:

$$\frac{\partial}{\partial x}(\rho U)+\frac{\partial}{\partial y}(\rho V)=0 \tag{1}$$

$$\frac{\partial}{\partial x}\left(\rho U^2\right)+\frac{\partial}{\partial y}(\rho VU)=\frac{\partial}{\partial x}\left(\mu\frac{\partial U}{\partial x}\right)+\frac{\partial}{\partial y}\left(\mu\frac{\partial U}{\partial y}\right)-\frac{\partial P}{\partial x} \tag{2}$$

$$\frac{\partial}{\partial x}(\rho UV)+\frac{\partial}{\partial y}\left(\rho V^2\right)=\frac{\partial}{\partial x}\left(\mu\frac{\partial V}{\partial x}\right)+\frac{\partial}{\partial y}\left(\mu\frac{\partial V}{\partial y}\right)-\frac{\partial P}{\partial y} \tag{3}$$

$$\frac{\partial}{\partial x}(\rho UT)+\frac{\partial}{\partial y}(\rho VT)=\frac{\partial}{\partial x}\left(\frac{k}{c_P}\frac{\partial U}{\partial x}\right)+\frac{\partial}{\partial y}\left(\frac{\mu}{\mathrm{Pr}}\frac{\partial T}{\partial y}\right) \tag{4}$$

where ρ is fluid density, U and V are the x and y velocity components, respectively, T is the temperature, μ is the dynamic viscosity and Pr is the Prandtl number. `

The modeled transport equations for the turbulent kinetic energy *k*, and its dissipation rate ε, respectively, are given by:

$$\frac{\partial}{\partial x}\left(\rho U k-\frac{\mu_t}{\sigma_k}\frac{\partial k}{\partial x}\right)+\frac{\partial}{\partial y}\left(\rho V k-\frac{\mu_t}{\sigma_k}\frac{\partial k}{\partial y}\right)=P_k-\rho\varepsilon \tag{5}$$

$$\frac{\partial}{\partial x}\left(\rho U \varepsilon-\frac{\mu_t}{\sigma_\varepsilon}\frac{\partial \varepsilon}{\partial x}\right)+\frac{\partial}{\partial y}\left(\rho V \varepsilon-\frac{\mu_t}{\sigma_\varepsilon}\frac{\partial \varepsilon}{\partial y}\right)=c_1\frac{\varepsilon}{k}P_k-c_2\rho\varepsilon \tag{6}$$

The symbols P_k and μ_t, respectively, represent the turbulence kinetic energy production rate and eddy viscosity, which are defined as:

$$P_k=\mu_t\left[2\left(\frac{\partial U}{\partial x}\right)^2+2\left(\frac{\partial V}{\partial y}\right)^2+\left(\frac{\partial U}{\partial y}+\frac{\partial V}{\partial x}\right)^2\right] \tag{7}$$

$$\mu_t=\rho c_\mu\frac{k^2}{\varepsilon} \tag{8}$$

Numerical Model The solution domain is divide into a number of rectangular control volumes (CV), resulting in a structure orthogonal non-uniform mesh. Grid points are locate according to a *cell-centered* scheme and velocities are store in a *collocated* arrangement (Patankar, 1980). A typical CV with its main dimensions and internodal distances is sketched in Figure 2. Writing equations (1)-(7) in terms of a general form

$$\frac{\partial}{\partial x}\left(\rho U\phi-\Gamma^\phi\frac{\partial \phi}{\partial x}\right)+\frac{\partial}{\partial y}\left(\rho V\phi-\Gamma^\phi\frac{\partial \phi}{\partial y}\right)=S^\phi \tag{9}$$

where ϕ stands for U, V, T, k or ε. The exchange coefficients Γ^ϕ and source terms S^ϕ for turbulent flow are compilated in Table 1. For the laminar flow the eddy viscosity and the turbulent Prantdl number are replaced by the corresponding molecular values, the k and ε-transport equations need not be solved.

Integrating the equation (9) over the control volume of Figure 2,

$$\int_{\delta V}\left[\frac{\partial}{\partial x}(\rho U\phi)+\frac{\partial}{\partial y}(\rho V\phi)\right]dv=\int_{\delta V}\left[\frac{\partial}{\partial x}\left(\Gamma^\phi\frac{\partial \phi}{\partial x}\right)+\frac{\partial}{\partial y}\left(\Gamma^\phi\frac{\partial \phi}{\partial y}\right)\right]dv+\int_{\delta V}S^\phi dv \tag{10}$$

Integration of three terms in (10), namely: convection, diffusion and source , lead to a set of algebraic equations. These practices are described elsewhere (e.g Patankar, 1980) and for this reason they not repeated here. In summary, convective terms are discretized using the upwind differencing scheme(UDS), diffusive fluxes make use of the central differencing scheme

Table 1 – Coefficients in the general transport equation (9).

ϕ	Γ^{ϕ}	S^{ϕ}
U	μ_t	$\frac{-\partial P}{\partial x}+\frac{\partial}{\partial x}\left(\mu_t\frac{\partial U}{\partial x}\right)+\frac{\partial}{\partial y}\left(\mu_t\frac{\partial V}{\partial x}\right)$
V	μ_t	$\frac{-\partial P}{\partial x}+\frac{\partial}{\partial x}\left(\mu_t\frac{\partial U}{\partial x}\right)+\frac{\partial}{\partial y}\left(\mu_t\frac{\partial V}{\partial x}\right)$
T	μ_t/Pr_t	S_T
k	μ_t/σ_k	$P_k-\rho\varepsilon$
ε	μ_t/σ_ε	$\frac{\varepsilon}{k}\left(c_1P_k-\rho c_2\varepsilon\right)$

Substitution of all approximate expressions for interface values and gradients into the integrated transport equation (10), gives the final discretization equation for grid node *P*

$$a_P\phi_P = a_E\phi_E + a_W\phi_W + a_N\phi_N + a_S\phi_S + b \tag{11}$$

with the east face coefficient, for example, being define as

$$a_E = \max\left[-C_e,0\right] + D_e \tag{12}$$

In (12) $D_e = \mu_e\delta_y / \Delta x_e$ and $C_e = \left(\rho U\right)_e\delta_y$ are the diffusive and convective fluxes at the CV east face, respectively, and , as usual, the operator max[a,b] returns the greater of a and b.

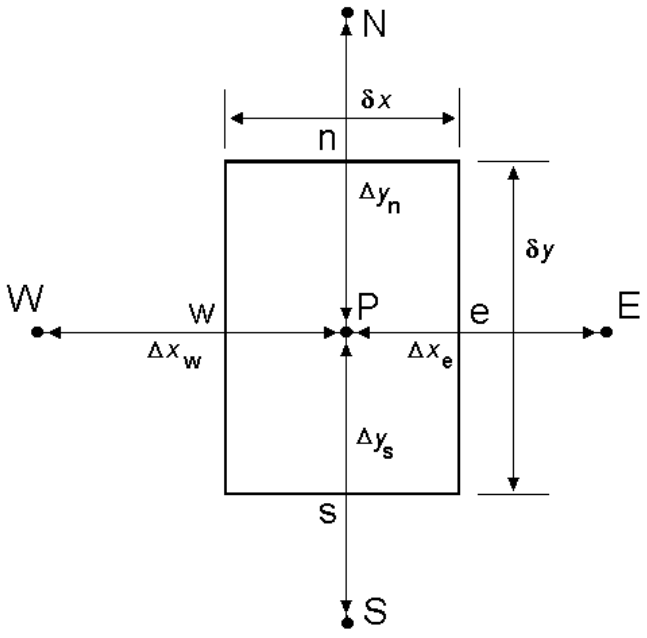

Figure 2 - Control Volume for Discretization

2.2. Multigrid Technique

Assembling equation (11) for each control volume of Figure 2 in the domain of Figure 1 defines a linear algebraic equation system of the form,

$$\mathbf{A}_k \mathbf{T}_k = \mathbf{b}_k \tag{13}$$

where $\mathbf{A}_k$ is the *matrix of coefficients*, $\mathbf{T}_k$ is the *vector of unknowns* and $\mathbf{b}_k$ is the vector accommodating source and extra terms. Subscript "k" refers to the grid level, with k=1 corresponding to the coarsest grid and k=M to the finest mesh.
defined as

As mentioned, multigrid is here implemented in a *correction storage* formulation (CS) in which one seeks coarse grid approximations for the *correction* defined as $\delta_k = \mathbf{T}_k - \mathbf{T}_k^*$ where $\mathbf{T}_k^*$ is an *intermediate value* resulting from a small number of iterations applied to (13). For a linear problem, one shows that δ_k is the solution of (Brandt, 1977, Stüben & Trottenberg, 1982, Hackbusch, 1985),

$$\mathbf{A}_k \delta_k = \mathbf{r}_k \tag{14}$$

where the *residue* is defined as

$$\mathbf{r}_k = \mathbf{b}_k - \mathbf{A}_k \mathbf{T}_k^* \tag{15}$$

Eq. (10) can be approximated by means of a coarse-grid equation,

$$\mathbf{A}_{k-1} \delta_{k-1} = \mathbf{r}_{k-1} \tag{16}$$

with the *restriction operator* I_k^{k-1} used to obtain

$$\mathbf{r}_{k-1} = I_k^{k-1} \mathbf{r}_k \tag{17}$$

The residue restriction is accomplished by summing up the residues corresponding to the four fine grid control volumes that compose the coarse grid cell. Thus, equation (17) can be rewritten as,

$$r_{k-1}^{I\,J} = r_k^{i\,j} + r_k^{i\,j+1} + r_k^{i+1\,j} + r_k^{i+1\,j+1} \tag{18}$$

Diffusive and convection coefficients in matrix $\mathbf{A}_k$ need also to be evaluated when changing grid level. Diffusive terms are recalculated since they depend upon neighbor grid node distances whereas coarse grid mass fluxes (*convective terms*) are simply added up at control volume faces. This operation , is commonly found in the literature (Peric, et al, 1989, Hortmann et al, 1990).

Once the coarse grid approximation for the correction δ_{k-1} has been calculated, the *prolongation* operator I_{k-1}^k takes it back to the fine grid as

$$\delta_k = I_{k-1}^k \delta_{k-1} \tag{19}$$

In order to update the intermediate value

$$\mathbf{T}_k = \mathbf{T}_k^* + \delta_k \tag{20}$$

Figure 3 illustrates a 4-grid iteration scheme for both the *V*- and *W*-cycles where the different operations are: *s=smoothing, r=restriction, cg=coarsest grid iteration* and *p=prolongation*. Also, the number of domain sweeps before and after grid change is denoted by ν^{pre} and ν^{post}, respectively. In addition, at the coarsest k level (k=1), the grid is swept ν^{cg} times by the error smoothing operator.

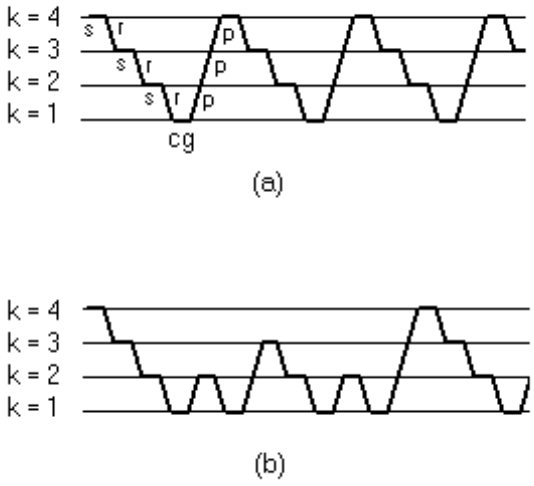

Figure 3 - Sequence of operations in a 4-grid iteration: (a) V-cycle; (b) W-cycle**.**

3. RESULTS AND DISCUSSION

The computer code developed was run on a IBM PC machine with a Pentium III 500MHz processor. Grid independence studies were conducted such that the solutions presented herein are essentially grid independent. For both V- cycles, pre- and post-smoothing iterations were accomplished via the Gauss-Seidel algorithm while, at the coarsest-grid, the TDMA method has been applied (Patankar, 1980). Also, the geometry of Figure 1 was run with the finest grid having sizes of 66x66 grid points.

Figure 4 shows non-dimensional temperature distribution patterns for flow in the heated tank flow of Figure 1. All walls are kept at the same temperature, higher than the incoming flow temperature. The figure indicates the effect of increasing the inlet Reynolds number, $Re_{in}=\rho U_{in}L_{in}/\mu$, where the subscript "in" refers to inlet values. One can clearly see the penetration of the cooler fluid as Re_{in} increases.

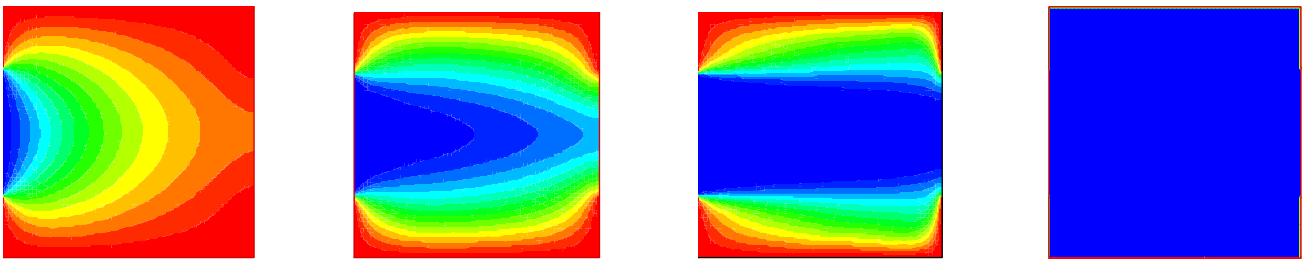

a) Re_{in} = 6 b) Re_{in} = 60 c) Re_{in} = 600 d) Re_{in} = 6000

Figure 4 - Temperature distribution patterns for flow in the heated tank flow

Residues. The residue is normalized and calculated according to

$$R_T = \sqrt{\sum_{ij} \left(R_{ij}^2 \right)}$$

$$\text{with} \quad R_{ij} = A_P T_P - \left(\sum_{nb} A_{nb} T_{nb} \right) \qquad \textbf{(21)}$$

where subscript *ij* identifies a given control volume on the finest grid and *nb* refers to its neighboring control volumes.

Figures 5 and 6 show the Turbulent kinetic energy and Dissipation of turbulent energy fields for turbulent flow for Re_{in} = 6000 and 60.000 respectively .One can see the effect of Re on the turbulent field.

Figure 7 shows residue history for the heated tank case. The solution follows a simultaneous approach in the sense that the temperature is always relaxed after the flow field, within the multigrid cycle. One can readily notice that for lower Re_{in}, regardless of the number of grids used, faster solutions are obtained. In this case, relative importance of diffusion term favors the stability of the system of equations. Increasing the number of grids for the same Reynolds number is also advantageous. This feature is what makes multigrid methods attractive, justifying their growing usage. However, it is also interesting to note that the computational effort related to value transfers among too many grids became relevant. In the figure, computational savings decrease as the number of grids increases.

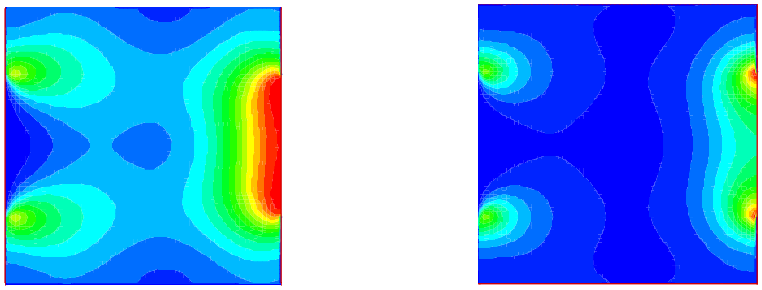

a) b)

Figure 5 - Turbulent kinetic energy (a) and Dissipation of turbulent energy (b) fields for turbulent flow for Re_{in} = 6000

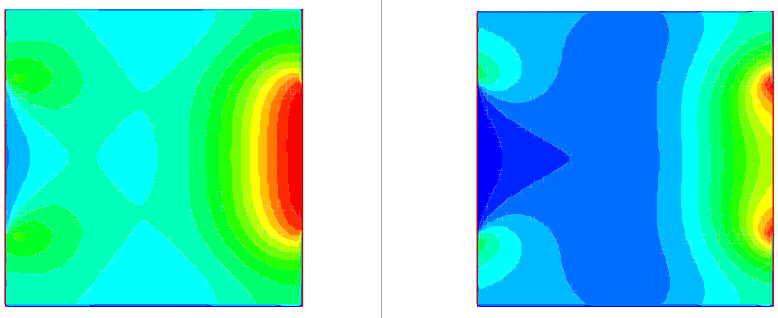

a) b)

Figure 6 - Turbulent kinetic energy (a) and Dissipation of turbulent energy (b) fields for turbulent flow for Re_{in} = 60000

Figure **8** presents residue history for the energy equation for the two situations considered, namely the simultaneous multigrid solution for velocity and temperature and the sole solution of the energy equation, given the flow field. As expected, the number of iterations needed in the latter case is lower, being nearly one order of magnitude less than in the former. Consequently, the advantage in using multiple grids is felt stronger in simultaneous solutions where overall computing time are greater.

Figure **9** reproduces the necessary time to convergence when the number of pre- and post-smoothing iterations was allowed to vary, keeping $\nu^{pre}=\nu^{post}$. One can see that more than one sweep for relaxing the intermediate solution, before and after grid change, brings no advantage to the algorithm performance and, consequently, further relaxation past this limit unnecessarily increases the computational effort. The advantage in using *W*-cycles is also apparent. When inspecting Figure one can see that, within a *W* cycle, the time spent per cycle on coarse grids is, on the average, greater than in *V*-cycles. Consequently, low frequency errors are more efficiently swept off (Rabi & de Lemos, 1998b). In addition, for the two values of ν^{cg} used (7 and 10), no detectable savings in computational time, for both cycles, are seen. That raises the question of how the value of ν^{cg} affects convergence performance as well.

In Figure **10** the number of pre- and post-smoothing iterations was fixed at $\nu^{pre}=\nu^{post}=2$ whereas the number of coarsest-grid sweeps ν^{cg} was free to vary. An optimum situation can be clearly identified for both cycles and further relaxation past this limit brings no time savings. Here again the superiority of the *W*-cycle is apparent.

Ultimately, both Figures **9** and **10** suggest a delicate balance between all parameters involved when minimum CPU consumption is sought. Most often, optimal parameters can not be easily determined *a priori* and adaptive strategies have been proposed in the literature. Generally, the ratio of residues after two successive sweeps is monitored and used as a criterion for switching grids. Hortmann *et al*, 1990 points out that this practice is preferred for single equation systems but, when solving the full equation set as done here, such practice is not easy to implement. In this case, most works in the literature specify a fixed number of sweeps, as in the cases here reported (Sathyamurthy & Patankar, 1994, Hutchinson *et al* 1988).

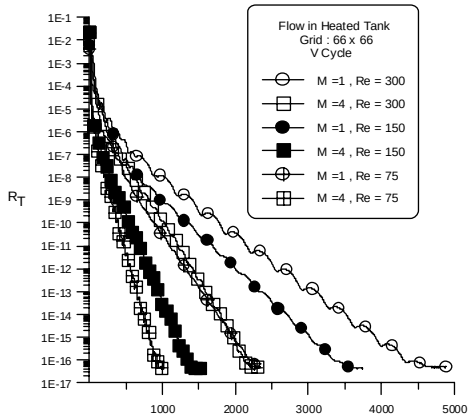

Figure 7 - Residue history for different Re_{in} – V- cycle.

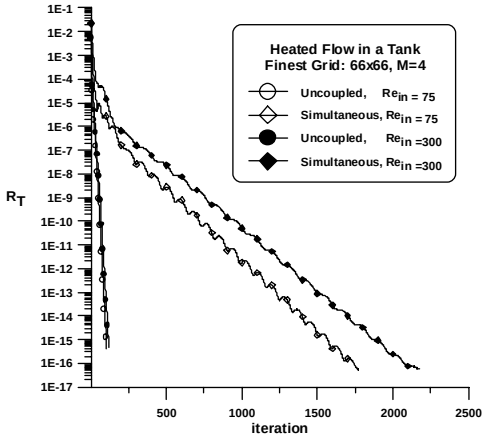

Figure 8 - Effect of field decoupling on residue history for temperature equation.

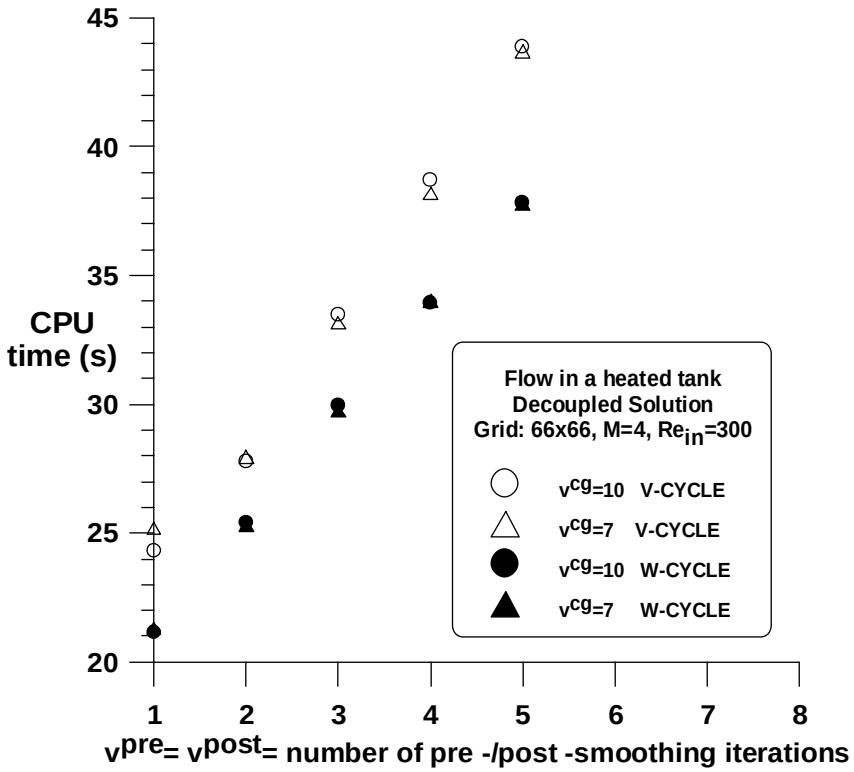

Figure 9 - Influence of the number of pre/post – smoothing iterations on the computational effort

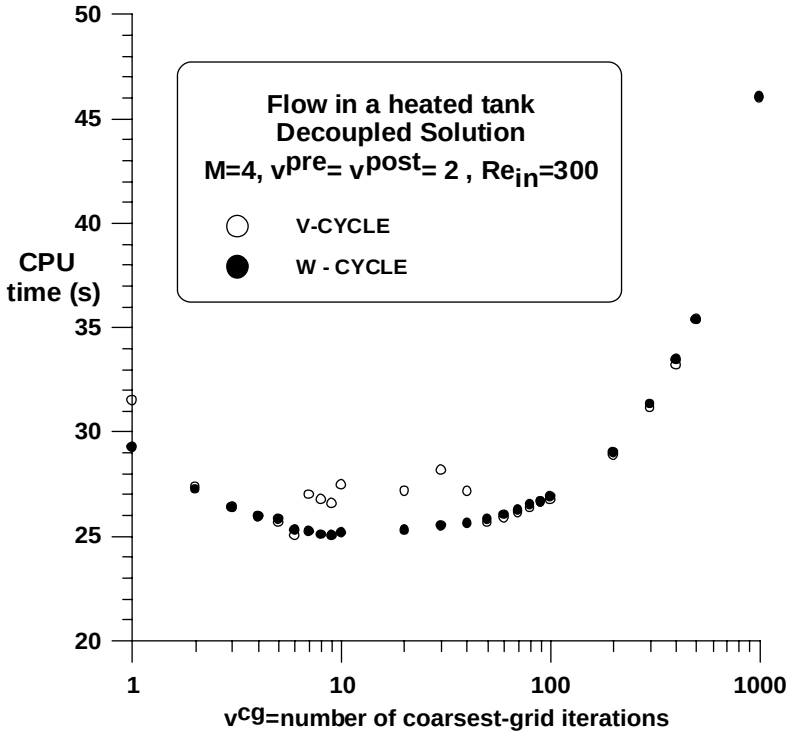

Figure 10 - Influence of the number of coarsest-grid iterations on the computational effort

4. AKNOWLEDGEMENTS

The authors are thankful to CNPQ, Brazil for their financial support during the course of this work.

5. REFERENCES

Brandt, A., 1977, Multi-Level Adaptive Solutions To Boundary-Value Problems, *Math. Comp.*, vol. 31, No. 138, pp. 333-390.

De Lemos, M.J.S., Mesquita, M.S., 1999a, Multigrid Numerical Solutions Of Non-Isothermal Laminar Recirculating Flows, *Applications of Computational Heat Transfer*, **ASME-HTD-vol. 364-3**, ISSN: 0272-5673, ISBN: 0-7918-1656-7, Ed..L.C. White, pg. 323-330.

Hackbusch, W., 1985, Multigrid Methods And Applications, Springer-Verlag, Berlin.

Hortmann, M., Peric, M., Scheuerer, G., 1990, Finite Volume Multigrid Prediction Of Laminar Convection: Bench-Mark Solutions, *Int. J. Num. Meth. Fluids*, vol. 11, pp. 189-207.

Hutchinson, B.R., Galpin, P.F., Raithby, G.D., 1988, Application Of Additive Correction Multigrid To The Coupled Fluid Flow Equations, *Num. Heat Transfer*, vol. 13, pp. 133-147.

Jiang, Y., Chen, C.P., Tucker, P.K., 1991, Multigrid solutions of unsteady Navier-Stokes equations using a pressure method, Num. Heat Transfer - part A, vol. 20, pp. 81-93.

Mesquita, M. S., de Lemos, M.J.S., 2000, Numerical Solution Of Non-Isothermal Laminar Recirculating Flows Using The Multigrid Method, Encit 2000, Porto Alegre, RS, Brazil, 2000.

Mesquita, M. S., de Lemos, M. J. S., 2000, Multigrid Numerical Solutions Of Laminar Back Step Flow, Congresso Nacional de Engenharia Mecânica, Natal, Rn, Brazil,2000.

Patankar S. V., Spalding D. B., 1972, A calculation procedure for heat, mass and momentum transfer in three-dimensional parabolic flows, Int. J.Heat Mass Transfer, Vol. 15, pp.1787-1806.

Patankar, S.V., 1980, Numerical Heat Transfer And Fluid Flow, Mc-Graw Hill.

Peric M., Rüger M., Scheurer G., 1989, A finite volume multigrid method for predicting periodically fully developed flow, Int. J. Num. Fluids, vol. 18, pp.843-852.

Peric, M., Rüger, M., Scheuerer, G., 1989, A Finite Volume Multigrid Method For Calculating Turbulent Flows, In: *Seventh Symposium on Turbulent Shear Flows*, pp. 7.3.1-7.3.6, Standford University.

Rabi, J.A., de Lemos, M.J.S., 1998a, Multigrid Numerical Solution Of Incompressible Laminar Recirculating Flows, Encit98- Proc. of 7th Braz. Cong. Eng. Th. Sci., vol. 2, pp. 915-920, Rio de Janeiro, RJ, Nov. 3-6.

Rabi, J.A., De Lemos, M.J.S., 1998b, The Effects Of Peclet Number And Cycling Strategy On Multigrid Numerical Solutions Of Convective-Conductive Problems, *7th AIAA/ASME Jnt Thermcs & HT Conf*, **Paper AIAA-98-2584**, Albuquerque, New Mexico, USA, June 15-18.

Rabi, J.A., De Lemos, M.J.S., 2001, "Optimization of convergence acceleration in multigrid numerical solutions of conductive-convective problems", Applied Math. Comp., Vol. 124, N. 2, pp. 215-226.

Raithby, G.D., Torrance, K.E., 1974, UPSTREAM-WEIGHTED DIFFERENCING SCHEMES AND THEIR APPLICATION TO ELLIPTIC PROBLEMS INVOLVING FLUID FLOW, *Comp. & Fluids*, vol. 2, pp. 191-206.

Sathyamurthy, P.S., Patankar, S.V., 1994, BLOCK-CORRECTION-BASED MULTIGRID METHOD FOR FLUID FLOW PROBLEMS, *Numerical Heat Transfer - Part B*, vol. 25, pp. 375-394.

Stüben, K., Trottenberg, U., 1982, MULTIGRID METHODS, In *Lect. Notes Math.*, vol. 960, pp. 1-76, Berlin

Thompson, M.C., Ferziger, J.H., 1989, An adaptive multigrid technique for the incompressible Navier-Stokes equations, *J. Comp. Phys.*, vol. 82, pp. 94-121.

Vanka, S.P. 1986, Block-implicit multigrid calculation of two-dimensional recirculating flows, *Comp. Meth. Appl. Mech. Eng.*, vol. 86, pp. 29-48.Bordalo, S.N., Ferziger, J.H. and Kline, S.J., 1989, "The Development of Zonal Models for Turbulence", Proceedings of the 10th Brazilian Congress of Mechanical Engineering, Vol. 1, Rio de Janeiro, Brazil, pp. 41-44.